ELSEVIER

Journal of Molecular Catalysis B: Enzymatic 19–20 (2003) 167–176

JOURNAL OF MOLECULAR CATALYSIS B: ENZYMATIC

www.elsevier.com/locate/molcatb

$[Cp^*Rh(bpy)(H_2O)]^{2+}$: a versatile tool for efficient and non-enzymatic regeneration of nicotinamide and flavin coenzymes

F. Hollmann, B. Witholt, A. Schmid*

Institute of Biotechnology, Swiss Federal Institute of Technology, ETH Hoenggerberg, HPT, CH-8093 Zürich, Switzerland

Received 27 September 2001; received in revised form 6 May 2002; accepted 20 May 2002

Abstract

$[Cp^*Rh(bpy)(H_2O)]^{2+}$ is a versatile tool for the non-enzymatic regeneration of oxidoreductase coenzymes such as NAD(P)H, $NAD(P)^+$, and $FADH_2$. The complex shows high stability and activity over a very broad range of pH (more than 60% activity between pH 3.5 and 9.7) and temperature (exponential increase of activity until at least 69 °C). The regeneration concept is not limited to sacrificial electron donors such as formate or alcohols for regeneration of reduced coenzymes; cheap electrical power as a reagent less source of reduction equivalents can also be used. At 30 °C, the complex has a specific activity of 1.2 U mg^{-1} for NAD(P)H regeneration and about 1 U mg^{-1} for $FADH_2$ regeneration with identical K_M values for both NAD^+ and $NADP^+$ of about 9 μM. In addition, a $[Cp^*Rh(bpy)(H_2O)]^{2+}$/FAD based concept for the regeneration of oxidized nicotinamide coenzymes is proposed.

Keywords: Coenzyme regeneration; Electrochemistry; In vitro; Oxidoreductase; Rhodium

1. Introduction

The in vitro application of oxidoreductases requires convenient and efficient coenzyme regeneration. Only a few examples have been reported where the production enzyme is regenerated directly, e.g. by direct electron transfer from the electrode to the active site [1]. In most cases, freely diffusible coenzymes like NAD(P) are inevitable for enzymatic activity. Their stochiometric application is economically unfeasible due to high costs or even impossible, as in case of flavins, where only the oxidized forms are commercially available. Furthermore, high concentrations of either form of the coenzymes can lead to enzyme inhibition necessitating catalytic amounts of the coenzymes and constant regeneration of the desired oxidation state.

General strategies have been reviewed recently [2–5] and comprise chemical, electrochemical, and enzymatic approaches. To date, enzymatic regeneration methods are preferred. For the regeneration of reduced nicotinamide coenzymes (NAD(P)H), for example, formate dehydrogenase (FDH, E.C. 1.2.1.2) has been studied extensively [6,7] and was used in various preparative scale applications [8]. This approach however suffers from the need for a second enzymatic system, moderate enzyme stability, and inflexibility with respect to different coenzymes.

Since in principle oxidoreductase coenzymes only switch between the oxidized and reduced state, electrochemical methods are appealing. Thus, for the regeneration of NAD(P)H or $FADH_2$ from their oxidized forms, the cathode as source of cheap reduction

* Corresponding author. Tel.: +41-1-633-3691; fax: +41-1-633-1051.
E-mail address: andreas.schmid@biotech.biol.ethz.ch (A. Schmid).

1381-1177/03/$ – see front matter
PII: S1381-1177(02)00164-9

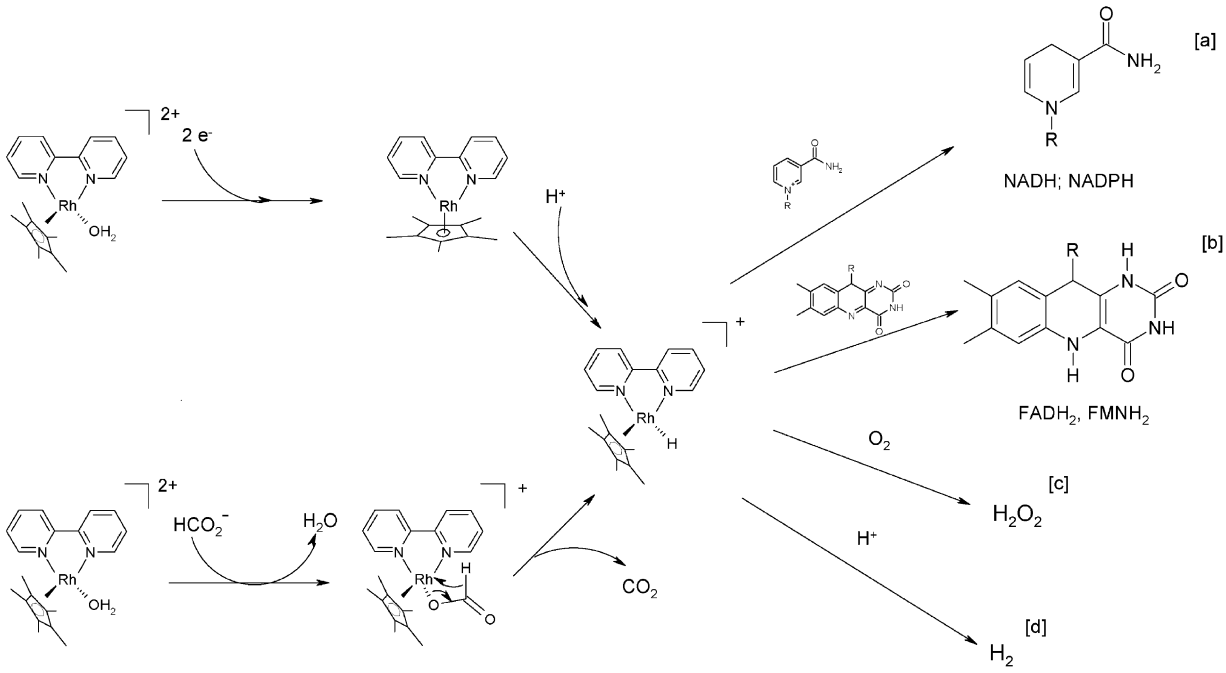

Fig. 1. Regeneration of the catalytically active $[Cp^*Rh(bpy)H]^+$ complex from $[Cp^*Rh^{III}(bpy)(H_2O)]^{2+}$ and possible applications. Literature: (a) [13,15–17]; (b) [18]; (c) [13]; (d) [14].

equivalents replaces the cosubstrates needed in enzymatic approaches [5].

Indirect electrochemical methods have been developed to avoid high overpotentials leading to undesired side reactions during direct cathodic $NAD(P)^+$ reduction. Viologenes were reported as electron shuttles between the cathode and a $NAD(P)^+$ reducing enzyme [9–11]. Yet, the toxicity of viologenes and the necessity for an enzyme transferring the reduction equivalents from viologene to $NAD(P)^+$ are disadvantageous. In addition, the regeneration reaction is quenched by molecular oxygen thus making this concept inapplicable to monooxygenase reactions [12].

Recently, we reported on the indirect electrochemical regeneration of a flavin-dependent monooxygenase utilizing pentamethylcyclopentadienyl rhodium bipyridine complexes ($[Cp^*Rh^{III}(bpy)(H_2O)]^{2+}$) [13] and demonstrated the general applicability of this enzyme-free regeneration concept (Fig. 1) for reduced nicotinamide coenzymes even in oxygen containing reaction mixtures thus allowing productive coupling to monooxygenases.

$[Cp^*Rh(bpy)H]^+$ acts as hydride transfer reagent not only on protons yielding H_2 [14] but also was shown to reduce some biologically active structures like nicotinamides [15–17], flavin analogues [18], or porphyrins [18,19]. The regeneration of the hydrido rhodium complex can be adjusted to the necessities of the enzymatic production system by utilizing either electrochemical methods [16] or “mild” chemical electron donors like formate [15] or alcohols [20].

In the present study, the $[Cp^*Rh(bpy)(H_2O)]^{2+}$ based regeneration concept for NAD(P)H is characterized with respect to parameters affecting its applicability to preparative-scale biotransformations and enlarged to an even broader range of possible applications in the field of bioinorganic chemistry.

2. Experimental

Unless indicated otherwise, all reagents were purchased from Fluka in the highest quality available and used without further purification.

2.1. Syntheses

[Cp*Rh(bpy)Cl]Cl was synthesized according to literature methods [14] in two steps: $RhCl_3 \cdot H_2O$ (Aldrich) is refluxed in methanol with one equivalent of hexamethyl Dewar benzene for 24 h. The resulting red precipitate is filtrated and suspended in methanol. On addition of two equivalents of 2,2′-bipyridine, the suspension clears up almost immediately and a yellowish solution is formed. From this, [Cp*Rh(bpy)Cl]Cl is precipitated on the addition of diethyl ether. Other complexes with substituted bipyridyl substituents are produced accordingly. Stock solutions (100 mM) are prepared in water and stored at room temperature. [Cp*Rh(bpy)Cl]Cl readily hydrolyzes to $[Cp^*Rh(bpy)(H_2O)]^{2+}$.

2.2. UV spectroscopy

$[Cp^*Rh(bpy)(H_2O)]^{2+}$ and FDH activity assays were performed on an Unicam UV-Vis spectrophotometer. The aqueous solution consisted of 50 mM potassium phosphate buffer (final volume 1 ml) with 150 or 500 mM sodium formate. The pH value was adjusted with phosphoric acid (85 wt.%) or potassium hydroxide (10 M), respectively. After supplementation with coenzymes to the indicated concentration, the sample was equilibrated at the desired temperature for at least 2 min. The assay was started by addition of FDH or $[Cp^*Rh(bpy)(H_2O)]^{2+}$, respectively. Unless indicated otherwise, the duration of the assay was 1 min and initial rates within the first 10 s were determined. In case of FAD reduction experiments, the buffers were degassed extensively with nitrogen prior to the assay. Nevertheless, traces of O_2 were still present in the solution and measurements were started when all O_2 was depleted by $FADH_2$ oxidation (seen by commencing decrease of absorption at 450 nm). NADH and FAD concentrations were determined using the extinction coefficients at 340 nm ($6220\ M^{-1}\ cm^{-1}$) and 450 nm ($12{,}000\ M^{-1}\ cm^{-1}$), respectively.

Michaelis–Menten constants (K_M values) were determined with Enzfitter (Elsevier-Biosoft, 1987).

NADH concentrations during electrolyses and preparative-scale reactions were determined spectrophotometrically after dilution to an appropriate absorption at 340 nm.

2.3. Electrochemical methods

All potentials are measured versus the saturated Ag/AgCl reference electrode (Cypress Systems, $E^0 = 195$ mV versus NHE).

Cyclic voltammetry was carried out as described previously [13] using a BAS-100B/W Electrochemical Analyzer (Bioanalytical Systems) utilizing a glassy carbon working electrode ($Ø = 3$ mm) and a Pt-wire counter electrode.

Potentiostatic electrolyses were performed in a thermostated 50 ml electrolysis cell. A cylindrical carbon felt electrode served as cathode. By placing the platinum counter electrode within a dialysis membrane a divided cell was obtained.

3. Results and discussion

3.1. Stability of $[Cp^*Rh(bpy)(H_2O)]^{2+}$

With respect to synthetic applications, the mediator stability is a crucial factor. Aqueous stock solutions of $[Cp^*Rh(bpy)(H_2O)]^{2+}$ were stored at room temperature. Under these conditions, no significant loss of catalytic activity was detected over several months. We, therefore, tested the complex under more extreme conditions, at 80 °C in acidic (pH 2), neutral, and basic (pH 12) phosphate buffers. At this temperature, the stability of mediator activity is a function of $[OH^-]$. At pH 12, the mediator activity showed a half-life time of 4.3 days which is somewhat higher at pH 7 (14.8 days). At pH 2, $[Cp^*Rh(bpy)(H_2O)]^{2+}$ maintained its full catalytic activity over more than 20 days. The loss of catalytic activity was accompanied by alterations of the spectroscopic properties of $[Cp^*Rh(bpy)(H_2O)]^{2+}$. With decreasing catalytic activity, the absorption maximum at 230 nm decreased (spectra not shown). We attribute this to the nucleophilic attack and substitution of the bipyridine ligand by OH^- at elevated temperatures. At 60 °C and neutral pH, no significant decrease of $[Cp^*Rh(bpy)(H_2O)]^{2+}$ activity was observed over more than 4 days and we conclude that $[Cp^*Rh(bpy)(H_2O)]^{2+}$ is very stable under common conditions for enzymatic synthesis (like $5 < pH < 10$ and $T < 80$ °C).

3.2. Reduction of nicotinamide (NAD(P)$^+$) and flavin (FAD) coenzymes

3.2.1. [Cp*Rh(bpy)(H$_2$O)]$^{2+}$ activity on NAD(P)$^+$ and FAD

[Cp*Rh(bpy)H]$^+$ can be obtained and regenerated from [Cp*Rh(bpy)(H$_2$O)]$^{2+}$ either by chemical or electrochemical procedures (Fig. 1). It acts as hydride transfer reagent on NAD(P)$^+$ yielding only the enzymatically active 1,4-NAD(P)H isomer. Recently, Fish and coworkers proposed a mechanism based on the coordination of ring-slipped η^3-Cp*Rh(bpy)H at the carbonyl-C-atom of oxidized NAD, thus explaining the exclusive generation of the 1,4-NAD(P)H isomer [21]. From this mechanism, two important features for the [Cp*Rh(bpy)H]$^+$ catalyzed regeneration of NAD(P)H can be derived. First, [Cp*Rh(bpy)H]$^+$ should display identical activities on NAD$^+$ and NADP$^+$ as the adenosine residue is not directly involved in the proposed coordination step. Second, on account of the "coordination pre-equilibrium" prior to the actual hydride transfer, a Michaelis–Menten like dependence of the regeneration reaction on the concentration of the oxidized coenzyme should be found. Kinetic measurements revealed the accuracy of both assumptions (Fig. 2). The K_M values for NAD$^+$ and NADP$^+$ were calculated to be 8.6 ± 1.2 and 9.6 ± 1.1 mM, respectively. Considering the limits of deviation, these values can be regarded as identical.

[Cp*Rh(bpy)H]$^+$ acts readily not only on nicotinamide but also on various other biologically active species like alloxazine-containing structures (Fig. 1). Since flavin coenzymes like FAD and FMN act as prosthetic groups for many monooxygenases [22], their regeneration is of preparative interest.

Nolte and coworkers reported catalytic activity of polymer modified [Cp*Rh(bpy)] complexes on *N*-methylalloxazine within lipid layers [18]. We, therefore, investigated the feasibility of the formate-driven FADH$_2$ regeneration catalyzed by [Cp*Rh(bpy)(H$_2$O)]$^{2+}$.

Fig. 3 illustrates the exponentially increasing catalytic activity of [Cp*Rh(bpy)(H$_2$O)]$^{2+}$ on both NAD$^+$ and FAD with increasing temperature. From the corresponding Arrhenius plots, the activation enthalpies for NAD$^+$ (76.9 kJ mol^{-1}) and FAD (91.7 kJ mol^{-1}) were calculated. As expected from the values for activation enthalpies, the mediator performance was somewhat lower for the reduction of FAD than for NAD(P)$^+$. Table 1 summarizes these results in terms of productivities for the formation of reduced coenzymes.

Since both NAD(P)H and FADH$_2$ regeneration rates are first order in the mediator concentration, the absolute production rate can easily be controlled via the concentration of [Cp*Rh(bpy)(H$_2$O)]$^{2+}$.

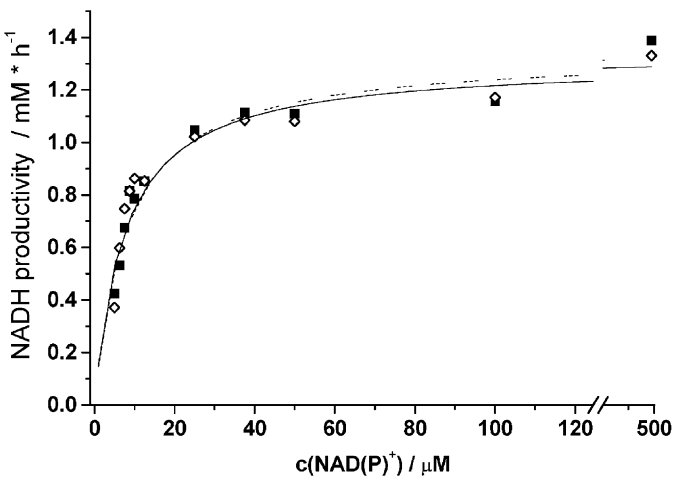

Fig. 2. Estimation of the Michaelis–Menten constants for NAD(P)$^+$: c([Cp*Rh(bpy)(H$_2$O)]$^{2+}$) = 4 mM, T = 30 °C; NADP$^+$ (■; ···), NAD$^+$ (◇; —).

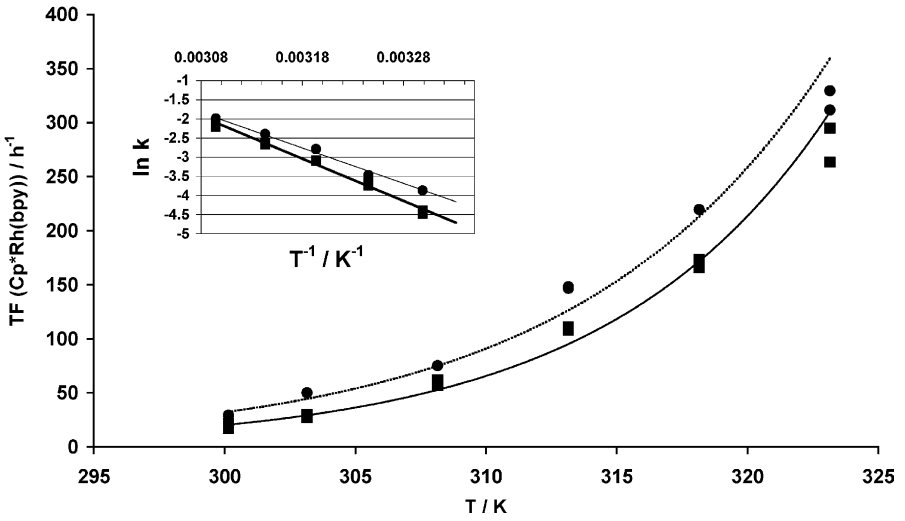

Fig. 3. Temperature dependence of $[Cp^*Rh(bpy)(H_2O)]^{2+}$ activity: NAD^+ (●) and FAD (■); 50 mM phosphate buffer (pH 7.5); $c(NaHCO_2) = 500$ mM; $c([Cp^*Rh(bpy)(H_2O)]^{2+}) = 25\,\mu M$; $c(FAD, NAD^+) = 0.25$ mM, degassed buffers were used in case of FAD reduction experiments; TF: turnover frequency (turnover rate); slight deviation of TF at elevated temperatures are due to insufficient thermal equilibrium; inset: Arrhenius plots for determination of activation enthalpies.

3.2.2. $[Cp^*Rh(bpy)(H_2O)]^{2+}$ activity as a function of pH

The activity range of $[Cp^*Rh(bpy)(H_2O)]^{2+}$ was elucidated with respect to the various pH optima of potential production enzymes. Fig. 4 displays the relative $[Cp^*Rh(bpy)(H_2O)]^{2+}$ activity towards NAD^+ under formate-driven regeneration conditions.

Between pH 3.8 and 8.5 $[Cp^*Rh(bpy)(H_2O)]^{2+}$ showed at least 80% of its maximum activity which lies at about pH 7. At higher proton concentrations, the NADH generation is predominantly inhibited by the proton-driven oxidation of $[Cp^*Rh(bpy)H]^+$ yielding H_2 whereas at high OH^- concentrations most probably $[Cp^*Rh(bpy)(OH)]^+$ is the predominant species (in comparable rhodium complexes a pK_A value of 8.2 was estimated for the coordinating water [20]) and ligand exchange with formate becomes rate limiting.

In order to elucidate the pH dependence of the electrochemical regeneration, $[Cp^*Rh(4\text{-methyl-bpy})(H_2O)]^{2+}$ dissolved in neutral and basic buffers was examined by cyclic voltammography (Fig. 5). At pH 7.5, the reduction peak potential was about 20 mV more positive than at pH 9 and no oxidation peak was observed whereas at pH 9 a distinctive desorptive oxidation peak appeared. This becomes evident when considering the proton uptake into the ligand sphere of reduced $[Cp^*Rh^I(bpy)]^0$ [17]. At sufficiently high proton concentrations, this chemical reaction occurs rapidly after the electrochemical steps and the catalytically active hydridorhodium complex is formed immediately. In the presence of NAD^+, catalytic peak current increases have been shown [13,17]. In basic media, this chemical reaction after the actual redox step becomes rate limiting and the uncharged

Table 1
Catalytic efficiency of $[Cp^*Rh(bpy)(H_2O)]^{2+}$

T (°C)	Productivity (mM h^{-1})		
	NADH	NADPH	$FADH_2$[a]
30	1.25	–	0.71
	3.70[b]	3.75[b]	–
40	3.68	–	2.74
50	8.02	–	6.98
69	29.78[b]	–	–

General conditions: $c([Cp^*Rh(bpy)(H_2O)]^{2+}) = 0.025$ mM, $c(NAD^+) = 1$ mM, $c(NaHCO_2) = 500$ mM.

[a] Degassed buffer.

[b] $c([Cp^*Rh(bpy)(H_2O)]^{2+}) = 0.1$ mM, $c(NaHCO_2) = 150$ mM, the formate-driven NADH regeneration rate is a function of both the mediator and the formate concentration [15].

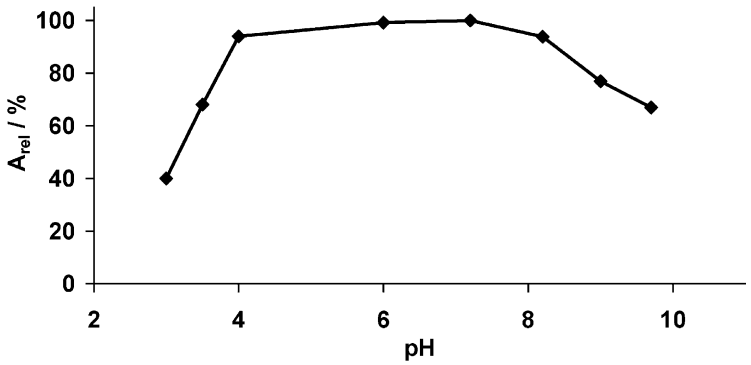

Fig. 4. Dependence of formate-driven NADH regeneration on pH: $c(NAD^+)_0 = 1\,mM$; $c([Cp^*Rh(bpy)(H_2O)]^{2+}) = 0.1\,mM$; $c(NaHCO_2) = 150\,mM$; $T = 30\,^\circ C$; the 100% value corresponds to a turnover frequency of $34.5\,h^{-1}$.

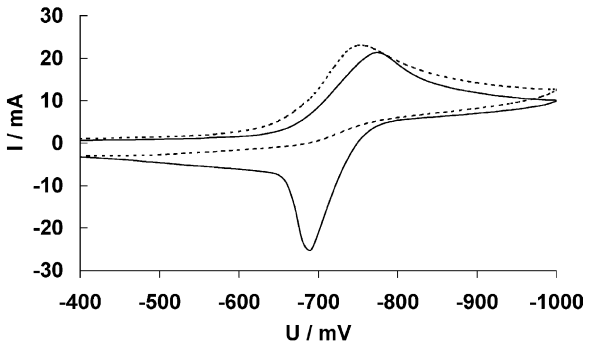

Fig. 5. Dependence of the electrochemical reduction of $[Cp^*Rh(bpy)(H_2O)]^{2+}$ on pH: $c([Cp^*Rh(4\text{-methyl-bpy})(H_2O)]^{2+}) = 0.5\,mM$ in degassed phosphate buffer (50 mM); pH 7.5 (···); pH 9 (—); scan rate $81\,mV\,s^{-1}$.

$[Cp^*Rh^I(bpy)]^0$ deposits on the electrode from where it is oxidatively released.

These effects were confirmed in preparative scale electrolyses in alkaline medium at pH 11.3. Shortly after applying a cathode potential of about −760 mV a rapid loss of mediator activity is observed, accompanied by a decrease in mediator concentration (determined by the absorption at 230 nm). After acidification (pH 2.2), both concentration and activity were restored and no significant decrease in the further course of the electrolysis was observed.

3.2.3. $[Cp^*Rh(bpy)(H_2O)]^{2+}$ activity as a function of ligands

Especially the formate-driven regeneration is strongly influenced by the kind and concentration of nucleophilic ligands. For example, 40 min pre-incubation of $[Cp^*Rh(bpy)(H_2O)]^{2+}$ in 50 mM $(NH_4)_2HPO_4$ buffer (pH 7) resulted in almost complete inhibition of the formate-driven NADH regeneration. Similar effects were observed in alkaline and in chlorine containing media or in TRIS buffers. These effects, however, influence the electrochemical regeneration to a far lesser extent. Cyclic voltammetry of $[Cp^*Rh(bpy)(H_2O)]^{2+}$ dissolved in 50 mM TRIS buffer for example revealed only a slightly more negative reduction peak potential (ca. 40 mV, data not shown). We confirmed this by preparative scale electrolyses (Table 2).

Table 2 clearly shows that strong ligands like ammonia inhibit the chemical regeneration whereas the

Table 2
Comparison of mediator activities as a function of buffer and electrode mass

Regeneration conditions	Cathode mass (g)	NADH productivity ($mM\,h^{-1}$)
Chemically	–	0.71[a]
	–	0.02[b]
Electrochemically[c]	0.6	0.55
	1.1	0.67
	1.7	0.75

General conditions: $c([Cp^*Rh(bpy)(H_2O)]^{2+}) = 0.02\,mM$, $c(NAD^+) = 0.4\,mM$, $T = 30\,^\circ C$.

[a] 50 mM potassium phosphate buffer (pH 7.5), $c(NaHCO_2) = 150\,mM$.

[b] 50 mM ammonium phosphate buffer (pH 7.5), $c(NaHCO_2) = 150\,mM$.

[c] 50 mM ammonium phosphate buffer (pH 7.5), $E = -750\,mV$.

electrochemical regeneration is dependent on diffusion limitation which can be overcome by optimizing the ratio of volume to electrode surface (represented by electrode mass).

The ligand exchange in case of the formate-driven NADH regeneration becomes rate limiting in the presence of strong coordinating ligands like NH_3, TRIS, or OH^-, thus strongly decreasing the NADH production rate. The electrochemical reaction, however, follows a somewhat different mechanism. Here, prior to the proton uptake, the metal center is reduced, forcing the monodental ligand out of the ligand sphere [17]. The electron donating effect of these ligands is reflected by the slightly more cathodic reduction potential.

Since enzymes are polypeptides containing lysine and other coordinating amino acid residues, an inhibition similar to the one described here could be assumed. Steckhan and coworkers, however, reported no decrease of $[Cp^*Rh(bpy)(H_2O)]^{2+}$ activity under formate-driven regeneration with several dehydrogenases [26]. Therefore, we assume that this effect is limited to proteins with free lysines at their surface.

3.2.4. *Influence of molecular oxygen on coenzyme regeneration*

As a substrate, molecular oxygen is a crucial factor in monooxygenase reactions. On the other hand, it reacts readily with numerous reduced molecules. For example, reduced viologenes that are the most common mediators in electrochemical NADH regeneration react very fast (limited only by diffusion) with molecular oxygen [12], which makes the use of these mediators for monooxygenase reactions impossible. For reduced rhodium complexes generated via alcohol oxidation, Kölle and Fränzel recently reported a rapid oxidation by molecular oxygen [20].

Our results confirm these findings only to some extent. A decrease in dissolved oxygen concentration during reduction of $[Cp^*Rh(bpy)(H_2O)]^{2+}$with formate was observed, while concomitantedly formation of hydrogen peroxide was detected. Strong aeration led to complete oxidation of $[Cp^*Rh(bpy)H]^+$ which can be followed by the color change from blue to yellow. However, at 30 °C the formate-driven NADH regeneration rate was not influenced. We found identical NADH production curves in degassed and aerated reaction mixtures. A slight attenuation was observed only at very low NAD^+ concentrations. In addition, formation of hydrogen peroxide was only found after a quantitative conversion of NAD^+ to NADH. This is in agreement with the very low K_M value determined for $NAD(P)^+$.

We found a somewhat stronger influence of molecular oxygen on the electrochemical regeneration of the hydridorhodium complex (Fig. 6). An initial NADH production rate of 0.53 mM h^{-1} was achieved in this typical example at an aeration rate of about 10 ml min^{-1}. NADH production, however, ceased on increase of the aeration rate to about 20 ml min^{-1} and recovered to 0.88 mM h^{-1} immediately after stopping external input of air.

Hydrogen peroxide, which is generated by direct cathodic reduction of O_2, can be excluded as oxidant inhibiting the electrochemical regeneration. Under formate-driven regeneration H_2O_2 pulses resulting in a more than 100-fold molar excess of H_2O_2 over $[Cp^*Rh(bpy)(H_2O)]^{2+}$ yielded no decrease of the NADH production rate. It can also be excluded that unprotonated $[Cp^*Rh^I(bpy)]^0$, a primary product of electrochemical reduction, exhibits higher oxygen sensitivity than the protonated form because formate-driven NADH regeneration at pH 9.7 also did not result in an alteration of NADH productivity upon strong aeration.

To date we are still lacking a plausible explanation for the ambivalent influence of oxygen on the formate-driven and the electrochemically driven NADH regeneration. The mechanism proposed by Kölle and Fränzel [20] includes a Rh(II) species that

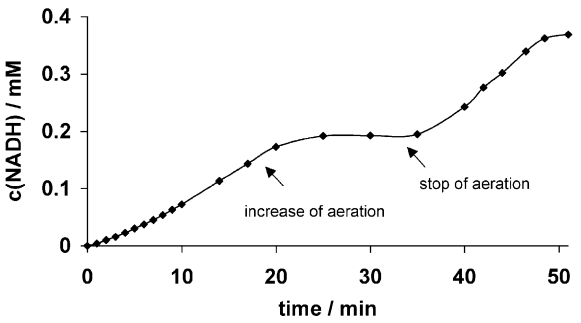

Fig. 6. Influence of O_2 on the electrochemical regeneration of NADH: 50 ml phosphate buffer (50 mM, pH 7.5); $c(NAD^+)_0 = 0.4$ mM; $c([Cp^*Rh(bpy)(H_2O)]^{2+}) = 0.02$ mM; $T = 30$ °C; $E = -750$ mV; arrows indicate increase and abortion of aeration.

also occurs during electrochemical reduction and is rather unlikely to be formed during formate-driven regeneration. Possibly, this Rh(II) species accounts for the higher oxygen sensitivity of the electrochemical NADH regeneration.

It should, however, be pointed out that the oxygen inhibition during electrochemically driven NADH regeneration can be controlled easily by the aeration rate. It is no grave obstacle in electro-enzymatic reactions because optimal conditions for both monooxygenase reaction and the regeneration reaction can be found.

3.2.5. Oxidation of NADH by $[Cp^*Rh(bpy)(H_2O)]^{2+}$

The hydride exchange between $NAD(P)^+$ and $[Cp^*Rh(bpy)H]^+$ is reversible. A decrease in NADH concentration was observed during incubation of NADH with oxidized $[Cp^*Rh(bpy)(H_2O)]^{2+}$ at pH 7.5. Yet, the high initial rate of NADH oxidation did not yield a constant NADH concentration as expected from a dynamic equilibrium reaction. Instead, the first reaction phase was followed by a slow oxidation of NADH over time, probably due to a slow re-oxidation of $[Cp^*Rh(bpy)H]^+$ (most probably via H^+). The initial NADH oxidation rate varied linearly with the complex concentration (data not shown) indicating a first order mechanism in $[Cp^*Rh(bpy)(H_2O)]^{2+}$. An activation enthalpy in the range of $46\,kJ\,mol^{-1}$ was estimated from temperature measurements. This activation enthalpy is significantly lower than the value we found for the hydride transfer to NAD^+ (Fig. 3), which may be explained by a contribution of re-aromatization energy.

This "reverse-reaction" is not desirable in electro-enzymatic reactions as it lowers the overall NADH production rate. Strongly binding ligands such as NH_3, however, prevent the $[Cp^*Rh(bpy)(H_2O)]^{2+}$ catalyzed oxidation of NADH. For example, 30 min pre-incubation of the rhodium complex in a 20 mM $(NH_3)_2HPO_4$ buffer (pH 7.5) inhibited the oxidation of NADH by 95%. Pre-incubation in 50 mM $(NH_3)_2HPO_4$ resulted in an almost undetectable rate of NADH oxidation. This may be explained by a coordination step prior to the actual hydride transfer step.

On the other hand, the "reverse-reaction" may be exploited for the regeneration of oxidized nicotinamide coenzymes. For this purpose, an efficient method to oxidize $[Cp^*Rh(bpy)H]^+$ has to be applied. On account of the very low stability of NAD(P)H in acidic media, regeneration of $[Cp^*Rh(bpy)(H_2O)]^{2+}$ via the reduction of protons is ruled out. A promising approach is to transfer the hydride equivalent to FAD and use molecular oxygen as terminal electron acceptor (Fig. 7).

We, therefore, tested the feasibility of this regeneration concept by incubating NADH with $[Cp^*Rh(bpy)(H_2O)]^{2+}$ and FAD alone and/or in combination of both (Fig. 8). Only the presence of both FAD and $[Cp^*Rh(bpy)(H_2O)]^{2+}$ resulted in a significant NADH oxidation rate. Within the first 10 min, this rate was $0.25\,mM\,h^{-1}$, corresponding to a mediator performance of 50.4 turnovers per hour. The subsequent decrease was due to NADH depletion in the reaction mixture, as successive analogous reactions were obtained after sequential addition of NADH (data not shown).

This regeneration concept has some synthetic potential as it represents an easily applicable and efficient method for regenerating oxidized nicotinamide coenzymes. Furthermore, expensive FAD can be replaced by cheaper alloxazine-based structures such as Vitamin B2 and others (data not shown). Molecular oxygen is a cheap and readily available terminal electron acceptor. For enzymatic reactions, where even low hydrogen peroxide concentrations are hazardous, electrochemical re-oxidation of $FADH_2$ is an option.

3.3. Comparison with other in vitro regeneration methods

As mentioned above, the regeneration system for reduced nicotinamide coenzymes used most commonly in preparative applications is based on FDH and formate. Relevant features of FDH and $[Cp^*Rh(bpy)(H_2O)]^{2+}$ are shown in Table 3.

$[Cp^*Rh(bpy)(H_2O)]^{2+}$ can compete with FDH as catalyst for NAD(P)H regeneration with respect to its pH range and its K_M values. The significantly smaller k_{cat} value (at 30 °C) is a typical property, when comparing metal catalysts with biological systems [23]. Yet, this is compensated by the specific activity at 30 °C and especially the high turnover rates at elevated temperatures. Furthermore, $[Cp^*Rh(bpy)(H_2O)]^{2+}$ displays a higher thermal stability and a broader substrate range (identical activities on NAD^+ and $NADP^+$ and a reasonable activity on FAD). Preliminary experiments showed that $[Cp^*Rh(bpy)(H_2O)]^{2+}$

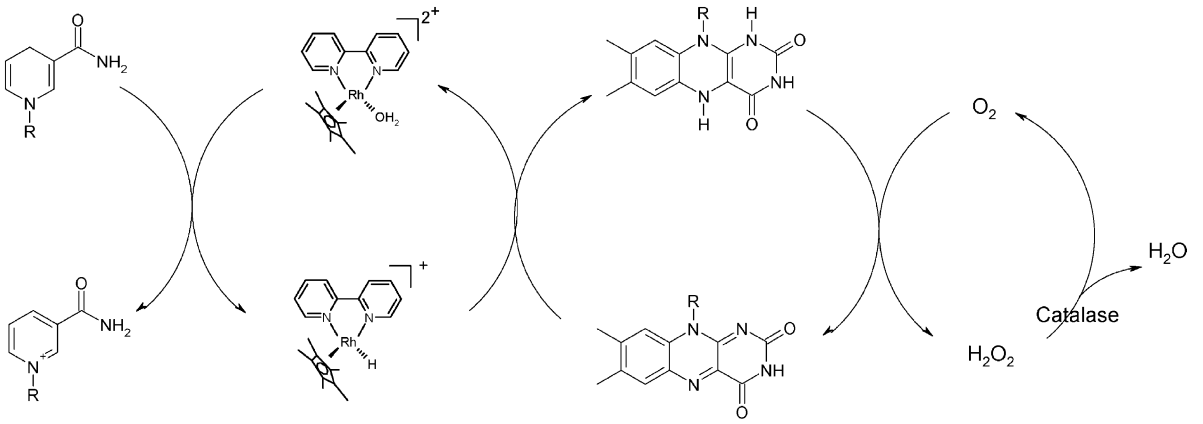

Fig. 7. A suggested regeneration system for $NAD(P)^+$ using $[Cp^*Rh(bpy)(H_2O)]^{2+}$/FAD.

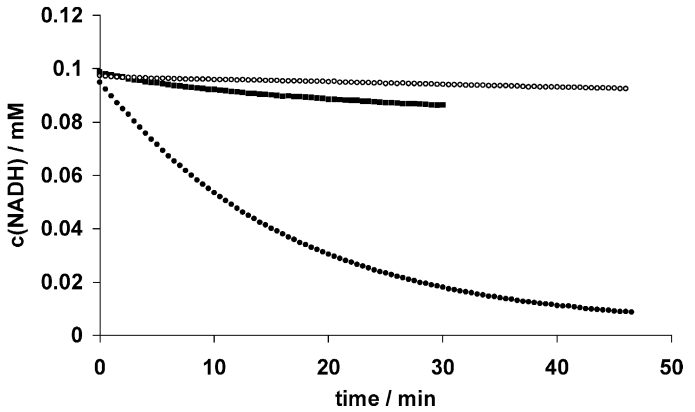

Fig. 8. Oxidation of NADH by $[Cp^*Rh(bpy)(H_2O)]^{2+}$/FAD: $c(NADH)_0 = 0.1$ mM; $T = 30\,^{\circ}C$; (■) only $[Cp^*Rh(bpy)(H_2O)]^{2+}$ (0.01 mM); (○) only FAD (0.04 mM); (●) both $[Cp^*Rh(bpy)(H_2O)]^{2+}$ (0.01 mM) and FAD (0.04 mM).

Table 3
Comparison of $[Cp^*Rh(bpy)(H_2O)]^{2+}$ with FDH

Kinetic parameter	$[Cp^*Rh(bpy)(H_2O)]^{2+}$	FDH from *candida boidinii*
K_M (NAD^+) (μM)	ca. 9[a]	90 [6]
K_M ($NaHCO_2$) (mM)	78	15 [6]
k_{cat} (NAD^+) (h^{-1})[b]	36	≈8400
Activity ($U\,mg^{-1}$)		
30 °C	1.2	2.4 [6]
69 °C	20	2.0[c]
Rel activity (%)[d]		
$NADP^+$	100	60 (mutant enzyme) [7]
FAD	≈80	Not detected
Temperature range	Exponential increase until at least 69 °C	Up to 55 °C [6]
pH range	>60% between 3.5 and 9.7	7.5–8.5 [6]

[a] Determined as described under Section 2.
[b] 150 mM $NaHCO_2$, 30 °C.
[c] At temperatures higher than 55 °C FDH activity decreased.
[d] Relative activity on NAD^+ (100%) under otherwise identical conditions.

can conveniently be separated from the reaction medium by cation exchangers and be recycled retaining its full activity (data not shown). In addition, the catalytically active $[Cp^*Rh(bpy)H]^+$ complex can be generated either chemically or electrochemically. We estimate the costs of 1 U (30 °C) $[Cp^*Rh(bpy)Cl]Cl$ to be in the range of 0.1€.

Compared to viologenes, the most common mediators for electrochemical NAD(P)H regeneration, $[Cp^*Rh(bpy)(H_2O)]^{2+}$ shows some major advantages, e.g. significantly less inhibition of the regeneration reaction by molecular oxygen and complete independence from an enzymatic step.

Concerning the regeneration of oxidized nicotinamides both enzymatic and electrochemical approaches have been reported. By catalyzing the hydride transfer from NADH to FMN by FMN reductase (with a 40-fold excess of FMN over NADH) turnover frequencies as high as $35\,s^{-1}$ for FMN reductase have been reported [24]. Ru–phenanthrolinedione complexes described by Steckhan and coworkers [25] generally exhibit performances in the range of 50–100 turnovers per hour (even though turnover frequencies of $1200\,h^{-1}$ have been reached). Consequently, the performance of our non-optimized regeneration system already lies within the same order of magnitude.

4. Conclusion

$[Cp^*Rh(bpy)(H_2O)]^{2+}$ is a versatile tool for the various regeneration needs of enzymatic redox reactions. It can be applied for the regeneration of oxidized and reduced nicotinamide coenzymes as well as reduced flavins. It is active over a broad pH and temperature range and convinces through its stability even under extreme conditions. Furthermore, the source of reduction equivalents can be chosen among cheap electrical power and chemical sources like formate or alcohols. Thus, $[Cp^*Rh(bpy)(H_2O)]^{2+}$ shows high potential for in vitro coenzyme regeneration for a broad variety of oxidoreductases.

Acknowledgements

We gratefully acknowledge financial support by the BASF Corporation (Ludwigshafen, Germany) and the ETH Zürich Research Commission (TH 24/99-3).

References

[1] V.L. Vilker, V. Reipa, M. Mayhew, M.J. Holden, J. Am. Oil Chem. Soc. 76 (1999) 1283.
[2] H.K. Chenault, G.M. Whitesides, Appl. Biochem. Biotechnol. 14 (1987) 147.
[3] P. Adlercreutz, Biocat. Biotrans. 14 (1996) 1.
[4] M.D. Leonida, Curr. Med. Chem. 8 (2001) 345.
[5] E. Steckhan, in: J. Bersier (Ed.), Topics in Current Chemistry, vol. 170, Springer, Berlin, 1994, pp. 84–111.
[6] V.O. Popov, V.S. Lamizin, Biochem. J. 301 (1994) 625.
[7] K. Seelbach, B. Riebel, W. Hummel, M.-R. Kula, V.I. Tishkov, A.M. Egorov, C. Wandrey, U. Kragl, Tetrahedron Lett. 37 (1996) 1377.
[8] A. Liese, K. Seelbach, C. Wandrey, Industrial Biotransformations, Wiley-VCH, Weinheim, 2000.
[9] A. Bergel, R. Devaux-Basseguy, J. Chim. Phys. 93 (1996) 753.
[10] W.A.C. Somers, W. Van Hartingsveldt, E.C.A. Stigter, J.P. van der Lugt, TiBTech 15 (1997) 495.
[11] H. Günther, A.S. Paxinos, M. Schulz, C. Van Dijk, H. Simon, Angew. Chem. 9 (1990) 1075.
[12] F. Rauwel, D. Thevenot, J. Electroanal. Chem. 75 (1977) 579.
[13] F. Hollmann, E. Steckhan, A. Schmid, Angew. Chem. Int. Ed. 40 (2001) 169.
[14] U. Kölle, B.-S. Kang, P. Infelta, P. Comte, M. Grätzel, Chem. Ber. 122 (1989) 1869.
[15] R. Ruppert, S. Herrmann, E. Steckhan, J. Chem. Soc. Chem. Commun. 17 (1988) 1150.
[16] R. Ruppert, S. Herrmann, E. Steckhan, Tetrahedron Lett. 28 (1987) 6583.
[17] E. Steckhan, S. Herrmann, R. Ruppert, E. Dietz, M. Frede, E. Spika, Organometallics 10 (1991) 1568.
[18] J.H. van Esch, M.A.M. Hoffmann, R.J.M. Nolte, J. Org. Chem. 60 (1995) 1599.
[19] P.A. Gosling, R.J.M. Nolte, J. Mol. Cat. A 113 (1996) 257.
[20] U. Kölle, H. Fränzel, Monatshefte f. Chem. 131 (2000) 1321.
[21] H.C. Lo, O. Buriez, J.B. Kerr, R.H. Fish, Angew. Chem. Int. Ed. 38 (1999) 1429.
[22] B.A. Palfey, V. Massey, in: M. Sinnott (Ed.), Comprehensive Biological Catalysis, vol. III, Academic Press, San Diego, 1998, pp. 83.
[23] A. Schmid, K. Hofstetter, H.-J. Feiten, F. Hollmann, B. Witholt, Adv. Synth. Cat. 343 (2001) 732.
[24] D.G. Drueckhammer, V.W. Riddle, C.-H. Wong, J. Org. Chem. 50 (1985) 5387.
[25] G. Hilt, B. Lewall, G. Montero, J.H.P. Utley, E. Steckhan, Liebigs Ann./Recueil (1997) 2289.
[26] D. Westerhausen, S. Herrmann, W. Hummel, E. Steckhan, Angew. Chem. Int. Ed. 31 (1992) 1529–1531.